J. Fluid Mech. (2008), *vol.* 595, *pp.* 163–172.
doi:10.1017/S0022112007009196 Printed in the United Kingdom

Electro-convection about conducting particles

EHUD YARIV[1] AND TOUVIA MILOH[2]

[1]Faculty of Mechanical Engineering, Technion – Israel Institute of Technology, Technion City 32000, Israel

[2]Department of Fluid Mechanics and Heat Transfer, Faculty of Engineering, Tel Aviv University, Ramat Aviv 69978, Israel

(Received 3 June 2007 and in revised form 18 October 2007)

A perfectly conducting spherical particle is suspended within an electrolyte solution and is exposed to a uniformly applied electric field. Using a weak-field approximation, the electro-kinetic flow is analysed for arbitrary Debye-layer thickness, the commonly employed thin-layer model emerging as a special case. We identify a scalar property which quantifies the global strength of the quadrupolar flow structure.

1. Introduction

In recent years there has been an increased interest in induced-charge electro-kinetic flows about polarizable particles. Unlike 'conventional' electro-kinetic flows (Saville 1977), which require the presence of an immobile surface-charge distribution, induced-charge flows can be driven even with initially uncharged particles. The prototypical scenario involves a perfectly conducting ion-impermeable particle which is suspended in an electrolyte solution. When an external electric field is applied, Faraday currents charge the region adjacent to its surface, thereby generating a polarized Debye layer. Simultaneously, the particle itself polarizes. The electric field exerts Lorentz body forces on its self-induced Debye cloud, thereby generating a velocity field (which is clearly nonlinear in the applied field intensity). This mechanism was explained in detail by Squires & Bazant (2004), who also clarified its relation to AC electro-osmosis (Ajdari 2000; Brown, Smith & Rennie 2000). Current interest in the induced-charge mechanism lies in microfluidic applications (Bazant & Squires 2004; Bazant & Ben 2006), animation of particle motion (Yariv 2005; Squires & Bazant 2006), and suspension dynamics (Saintillan, Darve & Shaqfeh 2006). A closely related field deals with the electrokinetic transport across ion-selective particle surfaces (Ben & Chang 2002).

Initial investigations of the induced-charge problem began in the former Soviet Union, usually for a spherical-particle geometry. The first analysis was carried out by Levich (1962) using a simplified capacitor model for the Debye layer. More rigorous investigations (Simonov & Dukhin 1973; Shilov & Simonova 1981) employed the thin-Debye-layer formulation. In that singular limit, the existence of the Debye layer is implicit in the boundary conditions which govern the electrically neutral fluid domain adjacent to it.

With the current focus in nanotechnology, one may encounter particles whose linear dimension is comparable with the Debye-layer thickness. In such situations, the thin-layer theoretical models require significant modification. Indeed, even the fundamental concepts of the thin-layer limit (e.g. zeta potential) lose their concrete meaning. While the thin-layer limit describes a slip-driven *electro-osmosis*, the general case of an arbitrary Debye thickness involves force-driven bulk *electro-convection* (see Rubinstein & Zaltzman 2001).

The problem of induced-charge flows for arbitrary (that is, not necessarily thin) Debye-layer thickness was partially addressed by Murtsovkin (1996), who analysed the nonlinear electro-kinetic transport about a spherical particle. The flow problem, however, was only solved in the thin-layer limit. The arbitrary-thickness problem was also investigated by Simonova, Shilov & Shramko (2001). That paper is mostly concerned with dielectrophoretic motion due to an externally imposed non-uniform electric field; the flow pattern that is driven by a uniform field component – which does not affect the dielectrophoretic velocity – was not fully resolved.

Our goal here is to present a systematic investigation of electro-kinetic flow about a conducting particle for arbitrary Debye thickness (wherein the thin-layer model will emerge as a special limit). We employ the prototypical configuration of a conducting spherical particle which is exposed to a uniform and constant externally imposed electric field. Unlike previous treatments we begin with the full Poisson–Nernst–Planck problem formulation, without making any *a priori* approximations. In dimensionless form, the governing equations are essentially affected by two parameters: the Debye thickness (normalized with particle size), and the applied field magnitude (normalized with the thermal-field scale). For nano- (and even micro-) scale particles, the latter parameter is usually small. We therefore conduct an asymptotic analysis in the limit of weakly applied fields. In this limit, the electrostatics and charge transport are decoupled from the flow, which itself is independent of the salt concentration profile. The flow field possesses the familiar quadrupolar structure of the thin-layer limit, but with a more complicated structure. We identify a new scalar parameter which quantifies the global flow intensity.

2. Problem formulation

Consider an initially uncharged spherical particle (radius a) which is suspended in an electrolyte solution (dynamic viscosity μ, kinematic viscosity ν, permittivity ϵ). The particle is a perfect conductor, and is chemically inert: its surface is impermeable to ions. We assume a symmetric $z-z$ binary solution; the concentrations of the cations and anions are then identical, say n_∞. For simplicity of presentation we also assume identical diffusivities, say D, of both ionic species. (Subsequent results do not require that assumption, but it is retained for brevity.)

At zero time, a uniform electric field E_∞ is externally applied. Within the initially homogeneous solution, field lines coincide with current lines. Thus, Ohmic currents (in conjunction with the particle impermeability to ions) generate an excess of anions at the particle 'front' ($x>0$) and cations at the particle 'back' ($x<0$), with the x-axis running parallel to the applied field and passing through the particle centre (at $x=0$). As this polarized Debye layer is established, a diffusive current develops so as to oppose Faradaic charging. Eventually, the system reaches a steady state, typically within a fraction of a second (see Squires & Bazant 2004). The action of the field upon the asymmetric charge distribution through Lorentz body forces results in the generation of flow, pumping fluid from the particle front and back and ejecting it along the plane $x=0$. In what follows, we focus upon the steady-state transport processes.

We employ a dimensionless notation which resembles that of Saville (1977). Length variables are normalized with a, the two ionic concentrations with n_∞, and the electric potential with the thermal scale $\varphi_T=kT/ze$ (kT being the Boltzmann factor, and e the elementary charge). Balancing Lorentz body forces with viscous stresses yields the velocity scale $\mathscr{U}=\epsilon\varphi_T^2/\mu a$. The pressure is normalized with $\mu\mathscr{U}/a$.

Assuming an incompressible flow, the ionic concentrations $n_\pm$ are governed by the conservation equations,

$$\nabla \cdot (\mp n_\pm \nabla\varphi - \nabla n_\pm) + Pe\, \boldsymbol{v} \cdot \nabla n_\pm = 0, \tag{2.1}$$

wherein $Pe = \mathscr{U} a/D$ is the Péclet number (which is $O(1)$ for typical ionic diffusivities). The three terms in (2.1) respectively represent ionic transport by electro-migration, diffusion, and convection. It is convenient to employ the reduced variables:

$$c = n_+ + n_-, \quad q = n_+ - n_-; \tag{2.2}$$

c is the total ionic concentration (normalized with n_∞), and q is the volumetric charge density (normalized with zen_∞). Addition of the two equations (2.1) yields the salt balance,

$$\nabla \cdot \boldsymbol{j} + Pe\, \boldsymbol{v} \cdot \nabla c = 0, \tag{2.3}$$

in which

$$\boldsymbol{j} = -q\nabla\varphi - \nabla c \tag{2.4}$$

is the total ionic flux (normalized with Dn_∞/a). Subtraction of the two equations (2.1) yields the charge balance,

$$\nabla \cdot \boldsymbol{i} + Pe\, \boldsymbol{v} \cdot \nabla q = 0, \tag{2.5}$$

wherein

$$\boldsymbol{i} = -c\nabla\varphi - \nabla q \tag{2.6}$$

is the current density (normalized with $zeDn_\infty/a$).

The electric potential φ is governed by Poisson's equation,

$$\lambda^2 \nabla^2 \varphi = -\frac{q}{2}, \tag{2.7}$$

wherein λ is the (dimensionless) Debye thickness:

$$\lambda^2 = \frac{\epsilon kT}{2z^2 e^2 a^2 n_\infty}. \tag{2.8}$$

The flow is governed by the Navier–Stokes equations:

$$\nabla \cdot \boldsymbol{v} = 0, \quad Re\, \boldsymbol{v} \cdot \nabla \boldsymbol{v} = -\nabla p + \nabla^2 \boldsymbol{v} + \nabla^2\varphi \nabla\varphi. \tag{2.9}$$

Here, $Re = \mathscr{U} a/\nu$ is the Reynolds number.

To prescribe the boundary conditions, it is convenient to employ a spherical-coordinate system, (r, θ, ϖ), centred about the sphere centre. The angle θ is measured from the symmetry axis x. The particle boundary is then given by the surface $r = 1$, and because of axial symmetry $\boldsymbol{v}$ adopts the form $\boldsymbol{e}_r u + \boldsymbol{e}_\theta v$. Since the particle is a perfect conductor, the electric potential possesses a uniform value at $r = 1$ which without loss of generality is taken to be zero. In addition, the impermeability to mass of the solid particle together with the no-slip condition imply that both u and v must vanish at the particle boundary. Since the particle is inert, the normal component of the ionic fluxes must also vanish, whence so must the radial components of $\boldsymbol{j}$ and $\boldsymbol{i}$:

$$q\frac{\partial\varphi}{\partial r} + \frac{\partial c}{\partial r} = c\frac{\partial\varphi}{\partial r} + \frac{\partial q}{\partial r} = 0 \quad \text{at} \quad r = 1. \tag{2.10}$$

Another condition at $r = 1$ represents a zero-net-charge constraint. The particle had no initial charge before the activation of the external field. During the unsteady

charging phase, following this activation, the particle became polarized by an amount consistent with the charging Debye cloud; however, its impermeability to ions implies that it cannot acquire any net charge. At steady state, the charge distribution at its boundary must therefore integrate to zero. Gauss's law, in conjunction with the vanishing electric field within the particle, readily yields the normalization condition,

$$\oint_{r=1} \mathrm{d}A \, \frac{\partial \varphi}{\partial r} = 0, \tag{2.11}$$

in which $\mathrm{d}A$ is a differential area element on the unit sphere.

At large distances from the particle the velocity field attenuates, $c \to 2$, and $q \to 0$. The electric field approaches the uniformly imposed field, whence

$$\varphi \sim -\beta r \cos\theta \quad \text{as} \quad r \to \infty. \tag{2.12}$$

Here

$$\beta = \frac{a E_\infty}{\varphi_T} \tag{2.13}$$

is the dimensionless applied-field magnitude.

3. Weak field analysis

Even when the external field is strong, β is usually a small parameter for sub-micron particles. As an example, consider a uni-valence aqueous solution ($\varphi_T \approx 0.025$ V): for $E_\infty = 100\ \mathrm{V\,cm^{-1}}$ and $a = 0.1\ \mu\mathrm{m}$, $\beta \approx 0.04$. Following Saville (1977), we perform an asymptotic analysis for $\beta \ll 1$. Note that in Saville's fixed-charge analysis, the external field perturbs an equilibrium Debye-layer static structure, which reflects the presence of adsorbed charge on the surface of a dielectric particle. In the present induced-charge analysis, on the other hand, the Debye cloud is a non-equilibrium phenomenon.

Since φ is driven by the externally imposed field (see (2.12)), it is $O(\beta)$. The Poisson equation (2.7) then implies that $q = O(\beta)$ as well. From the ionic-balance equation (2.3) and the far-field limit of c we find that $c = 2 + O(\beta^2)$. Thus, $\boldsymbol{i} = O(\beta)$. The momentum balance (2.9) implies that both $\boldsymbol{v}$ and p are $O(\beta^2)$. We therefore introduce the following re-scaling:

$$\varphi = \beta \Phi, \quad q = \beta Q, \quad c = 2 + \beta^2 C, \quad \boldsymbol{i} = \beta \boldsymbol{I}, \quad \boldsymbol{v} = \beta^2 \boldsymbol{V}, \quad p = \beta^2 P. \tag{3.1}$$

In what follows, we perform a leading-order analysis in the limit $\beta \to 0$. The fields Φ and Q satisfy the differential equations,

$$\lambda^2 \nabla^2 \Phi = -\frac{Q}{2}, \tag{3.2}$$

$$\nabla^2 Q + 2\nabla^2 \Phi = 0, \tag{3.3}$$

whence the electrostatics and charge-transport problems are decoupled from those governing C and the flow. They also satisfy the boundary conditions at $r = 1$,

$$\Phi = 0, \tag{3.4}$$

$$2\frac{\partial \Phi}{\partial r} + \frac{\partial Q}{\partial r} = 0, \tag{3.5}$$

the zero-net-charge constraint,

$$\oint_{r=1} \mathrm{d}A \, \frac{\partial \Phi}{\partial r} = 0. \tag{3.6}$$

and the far-field conditions

$$\Phi \sim -r\cos\theta, \quad Q \to 0. \tag{3.7}$$

Once Φ and Q are evaluated, the flow field can be calculated. The solenoidal velocity field $\boldsymbol{V}$ satisfies the inhomogeneous Stokes equation

$$\nabla P = \nabla^2 \boldsymbol{V} - \frac{1}{2\lambda^2} Q \nabla \Phi. \tag{3.8}$$

In addition, it vanishes at $r = 1$ and decays as $r \to \infty$.

Note that there is no need to solve for C (which satisfies an inhomogeneous Neumann-type problem). Also, convection of both ions and momentum do not appear in the preceding leading-order analysis. Since it is only in these convection terms that the difference between the two ionic diffusivities appears (through two different Péclet numbers), it becomes evident that the (artificial) assumption of identical ionic diffusivities does not affect the validity of subsequent analysis.

3.1. *Charge, potential, and current*

From the charge balance (3.3) we find that

$$Q = -2\Phi + \chi, \tag{3.9}$$

where χ is a harmonic function. Substitution into (3.5) and making use of (3.7) shows that χ satisfies the following boundary conditions:

$$r = 1: \quad \frac{\partial \chi}{\partial r} = 0, \tag{3.10}$$

$$r \to \infty: \quad \chi \sim -2r\cos\theta. \tag{3.11}$$

Accordingly,

$$\chi = -2\left(r + \frac{1}{2r^2}\right)\cos\theta + \alpha, \tag{3.12}$$

where α is an integration constant which remains to be determined.†

To understand the physical meaning of χ, consider the current density:

$$\boldsymbol{I} = -2\nabla\Phi - \nabla Q. \tag{3.13}$$

Comparing with (3.9), we see that χ constitutes a current potential:‡

$$\boldsymbol{I} = -\nabla\chi. \tag{3.14}$$

Thus, Laplace's equation which governs χ is simply an expression of the leading-order charge conservation (cf. (2.5)):

$$\nabla \cdot \boldsymbol{I} = 0, \tag{3.15}$$

† Naively, it may appear that α could be set to any arbitrary value. However, χ is related to Q (whose zero-level cannot be manipulated) through Φ, whose zero-level was already set in the boundary condition (3.4). Prescribing a value for α is therefore equivalent to an over-specification of the problem.

‡ In the general $\beta = O(1)$ case the current density is not necessarily a conservative vector field.

and the no-flux condition (3.10) represents the impermeability of the particle to electric current.

Substituting (3.9) into the Poisson equation (3.2) yields the Helmholtz equation,

$$\lambda^2 \nabla^2 Q = Q, \tag{3.16}$$

while the equi-potential condition (3.4) yields the Dirichlet boundary condition

$$Q(r=1) = \alpha - 3\cos\theta. \tag{3.17}$$

The solution of (3.16)–(3.17) which decays at large r is

$$Q = \mathrm{e}^{(1-r)/\lambda}\left(\frac{\alpha}{r} - \frac{3}{r^2}\frac{\lambda+r}{\lambda+1}\cos\theta\right). \tag{3.18}$$

Substitution into (3.9) yields

$$\Phi = f(r)\cos\theta - \frac{\alpha}{2r}\mathrm{e}^{(1-r)/\lambda} \tag{3.19}$$

where

$$f(r) = \frac{3}{2r^2}\frac{\lambda+r}{\lambda+1}\mathrm{e}^{(1-r)/\lambda} - r - \frac{1}{2r^2} + \frac{\alpha}{2}. \tag{3.20}$$

Use of the zero-charge condition (3.6) readily yields $\alpha = 0$. Clearly, α is proportional to the initial charge possessed by the particle. As expected, the polarized charge distribution describes an excess of positive ions at the particle back ($x < 0$) and negative ions at its front ($x > 0$). Our results are in agreement with those of Murtsovkin (1996).

3.2. *Current and field lines*

In the thin-Debye-layer limit, the electric-field lines coincide with the current lines. Due to the presence of bulk diffusion currents, this is not the case in the present analysis, and it it illustrative to depict both families. Since the electric current is solenoidal (see (3.15)), and given the axisymmetry of the problem, the current lines can be constructed using a stream-function-type formulation (Happel & Brenner 1965). We define a 'current function' τ via the relation:

$$\boldsymbol{I} = \frac{1}{r\sin\theta}\,\boldsymbol{e}_{\varpi} \times \nabla\tau. \tag{3.21}$$

With this definition, curves of constant τ coincide with the current lines, which are everywhere parallel to $\boldsymbol{I}$. Use of (3.12)–(3.14) and (3.21) readily yields

$$\tau = r^2\sin^2\theta\left(1 - \frac{1}{r^3}\right). \tag{3.22}$$

Note that the current lines, unlike the electric-field lines, are independent of λ, and are therefore identical to those in the thin-layer limit.

It is also desired to obtain an analytic expression for the electric-field lines $G(r,\theta) = \text{constant}$. These lines are orthogonal to the equi-potential lines, whence ∇G is everywhere perpendicular to $\nabla\Phi$. This condition is satisfied by the form $G(r,\theta) = g(r)\sin\theta$ wherein

$$g(r) = \exp\int_1^r \frac{f(s)}{s^2 f'(s)}\mathrm{d}s. \tag{3.23}$$

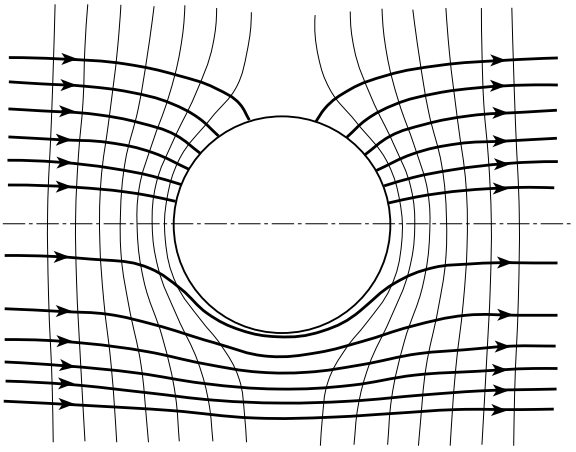

FIGURE 1. Equi-potential lines (thin), electric-field lines (upper portion), and current lines (lower portion) at the meridian plane for $\lambda = 1$. The external field is directed from left to right.

(Since the electric field is non-solenoidal, G cannot be determined using a stream-function formulation.)

The equi-potential lines ($\Phi =$ constant), current lines ($\tau =$ constant), and field lines ($G =$ constant) are depicted in figure 1 for $\lambda = 1$. The field lines, which must intersect the surface $r = 1$ at right angles (see (3.4)), are shown at the upper portion of the figure. The current lines, which are expelled from the particle, are shown at the lower portion.

4. Flow field

Since $\boldsymbol{V}$ is solenoidal, the momentum equation (3.8) can be recast in the form

$$\nabla P = -\nabla \times \boldsymbol{\omega} - \frac{1}{4\lambda^2} Q(\nabla\chi - \nabla Q). \tag{4.1}$$

where $\boldsymbol{\omega} = \nabla \times \boldsymbol{V}$ is the fluid vorticity. Forming the curl of this equation yields the vorticity equation:

$$\nabla \times (\nabla \times \boldsymbol{\omega}) = -\frac{1}{4\lambda^2} \nabla Q \times \nabla\chi. \tag{4.2}$$

Since $\boldsymbol{V}$ is axisymmetric, it may be obtained from a Stokes stream function ψ:

$$\boldsymbol{V} = \frac{1}{r\sin\theta} \boldsymbol{e}_{\varpi} \times \nabla\psi. \tag{4.3}$$

Then, the left-hand side of (4.2) may be expressed in terms of ψ:

$$\nabla \times (\nabla \times \boldsymbol{\omega}) = -\boldsymbol{e}_{\varpi} \frac{\mathrm{E}^4\psi}{r\sin\theta}. \tag{4.4}$$

Here

$$\mathrm{E}^2 = \frac{\partial^2}{\partial r^2} + \frac{\sin\theta}{r^2} \frac{\partial}{\partial\theta} \left(\frac{1}{\sin\theta} \frac{\partial}{\partial\theta} \right). \tag{4.5}$$

Substitution of (3.12)–(3.20) and (4.4) into the vorticity equation (4.2) yields the inhomogeneous equation for ψ:

$$\mathrm{E}^4\psi = \frac{3}{\lambda^3(1+\lambda)}\mathrm{e}^{(1-r)/\lambda}\left(1+\frac{3\lambda}{r}+\frac{3\lambda^2}{r^2}+\frac{1}{2r^3}\right)\mathscr{C}_3^{-1/2}(\cos\theta). \tag{4.6}$$

Here, $\mathscr{C}_3^{-1/2}(\eta) = \eta(1-\eta^2)/2$ is the Gegenbauer function of order 3 and degree $-1/2$. This equation is to be solved subject to a zero-velocity condition at the particle surface,

$$r = 1: \quad \psi = \frac{\partial\psi}{\partial r} = 0, \tag{4.7}$$

and at large distances,

$$r \to \infty: \quad \psi/r^2 \to 0. \tag{4.8}$$

We seek a solution which possesses the quadrupolar structure,

$$\psi = h(r)\mathscr{C}_3^{-1/2}(\cos\theta). \tag{4.9}$$

Substitution into (4.6) yields the following ordinary differential equation for $h(r)$:

$$\frac{\mathrm{d}^4h}{\mathrm{d}r^4} - \frac{12}{r^2}\frac{\mathrm{d}^2h}{\mathrm{d}r^2} + \frac{24}{r^3}\frac{\mathrm{d}h}{\mathrm{d}r} = \frac{3}{\lambda^3(1+\lambda)}\left(1+\frac{3\lambda}{r}+\frac{3\lambda^2}{r^2}+\frac{1}{2r^3}\right)\mathrm{e}^{(1-r)/\lambda}. \tag{4.10}$$

This equation is solved subject to the vanishing of h and its derivative at $r = 1$, together with the requirement that h is $o(r^2)$ at large r. The solution is

$$\begin{aligned}(1+\lambda)h(r) = {} & \frac{3\lambda}{2}+\frac{3}{2}+\frac{1}{20\lambda^2}+\frac{9-7\lambda}{160\lambda^4}+\frac{\lambda-1}{320\lambda^6}+\mathrm{e}^{(1-r)/\lambda}\left(\frac{3}{70r^2}+\frac{9\lambda^3}{r^2}+\frac{3}{70\lambda r}+\frac{9\lambda^2}{r}\right.\\ & \left.+3\lambda-\frac{1}{35\lambda^2}+\frac{11r\lambda-13r^2}{560\lambda^4}+\frac{r^4-\lambda r^3}{1120\lambda^6}\right)+\frac{1}{r^2}\left(\frac{1-\lambda}{448\lambda^6}+\frac{27\lambda-37}{1120\lambda^4}\right.\\ & \left.-\frac{3}{140\lambda^2}-\frac{3}{70\lambda}-\frac{54}{35}-\frac{9\lambda}{2}-9\lambda^2-9\lambda^3\right)+\mathrm{e}^{1/\lambda}\left[E_1(r/\lambda)\left(\frac{r^3}{40\lambda^5}-\frac{r^5}{1120\lambda^7}\right)\right.\\ & \left.+E_1(1/\lambda)\left(\frac{1}{320\lambda^7}-\frac{1}{448\lambda^7r^2}-\frac{1}{16\lambda^5}+\frac{3}{80\lambda^5r^2}\right)\right],\end{aligned} \tag{4.11}$$

wherein $E_1(s) = \int_s^\infty \mathrm{e}^{-t}/t\,\mathrm{d}t$ is the exponential integral. The streamlines $\psi =$ constant for $\lambda = 1$ are depicted in figure 2(*a*). Evaluation of h for other λ values indicates that the quadrupolar flow pattern possesses the same attributes as its thin-layer counterpart, namely open-ended streamlines without stagnation points.

The solution (4.9) describes a flow mechanism which pumps liquid from the regions about the $\theta = 0$ (fore) and $\theta = \pi$ (aft) axes and ejects it along the $\theta = \pi/2$ equatorial plane. (Indeed, such flows were suggested by Bazant & Squires (2004) to be used as microfluidic pumps.) These regions can be precisely defined: from (4.9), it is evident that the radial velocity vanishes for $\theta = \theta_0$ and $\theta = \pi - \theta_0$, where $\cos\theta_0 = 1/\sqrt{3}$ ($\theta_0 \cong 54.7^\circ$). The regions of inflow are within the 'front cone' $\theta < \theta_0$ and the 'back cone' $\theta > \pi - \theta_0$. The region of outflow is $\theta_0 < \theta < \pi - \theta_0$.

Here, we propose using a new scalar estimate of the 'pumping rate', to be defined as the net volumetric flux F (normalized with $\beta^2a^2\mathscr{U}$) which enters the back cone at large distances from the particle. Given the flux-measure property of the stream

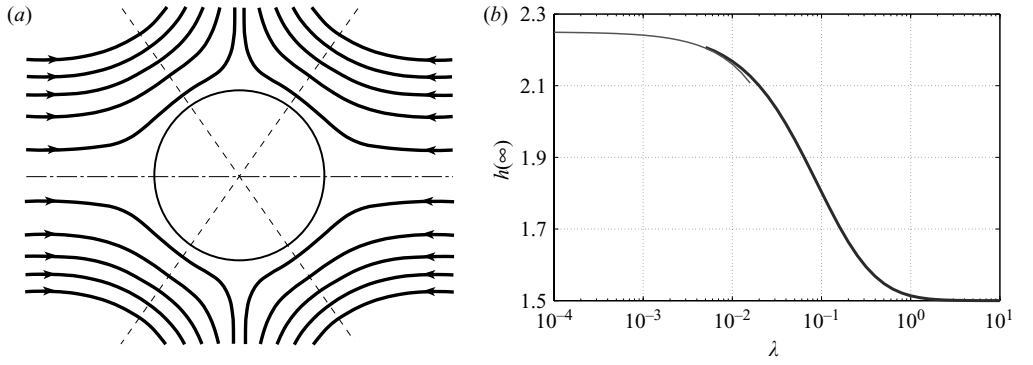

FIGURE 2. (*a*) Streamlines (ψ = constant) at the meridian plane for $\lambda = 1$, drawn using (4.9) and (4.11). Also shown are the front ($\theta = \theta_0$) and back ($\theta = \pi - \theta_0$) 'in-flow' cones. (*b*) The dependence of $h(\infty)$ upon λ. The thick line is calculated from (4.13) and the thin line represents the asymptotic approximation (4.15).

function, F is given by the limit

$$F = -2\pi \lim_{r\to\infty} \psi(r, \pi - \theta_0) = \frac{2\pi}{3^{3/2}} h(\infty). \tag{4.12}$$

The dependence of F upon the Debye thickness λ is embodied in $h(\infty)$. From (4.11) we find that

$$(1+\lambda)h(\infty) = \frac{3\lambda}{2} + \frac{3}{2} + \frac{1}{20\lambda^2} - \frac{7}{160\lambda^3} + \frac{9}{160\lambda^4} + \frac{1}{320\lambda^5} - \frac{1}{320\lambda^6} + \mathrm{e}^{1/\lambda} E_1(1/\lambda)\left(\frac{1}{320\lambda^7} - \frac{1}{16\lambda^5}\right). \tag{4.13}$$

It is of interest to evaluate F in the respective limits of thin and thick Debye layers. In the thin-layer limit, $\lambda \ll 1$, it may appear from (4.13) that $h(\infty)$ (and hence F) diverges. However, from the asymptotic relation (Abramowitz & Stegun 1965, p. 231)

$$\mathrm{e}^{1/\lambda} E_1(1/\lambda) \sim \lambda \sum_{n=0}^{\infty} (-1)^n n!\, \lambda^n, \quad \lambda \to 0, \tag{4.14}$$

we find (this requires taking at least six terms in (4.14)) that $h(\infty)$ approaches a finite limit:

$$h(\infty) \sim \frac{9}{4} - \frac{27\lambda}{4} + O(\lambda^2), \quad \lambda \to 0. \tag{4.15}$$

The value 9/4 agrees with the thin-Debye-layer limit (Murtsovkin 1996). The thick-layer limit, $h(\infty) \sim 3/2 + O(1/\lambda)$, is trivial to obtain. The dependence of $h(\infty)$ upon λ is shown in figure 2(*b*).

5. Concluding remarks

A uniform and constant electric current through an electrolyte salt solution is associated with two streams of positive and negative ions in a stationary neutral liquid. When an ion-impermeable particle is suspended in the solution, it perturbs both streams. The resulting ionic-transport process generates a polarized Debye layer about the particle boundary. The electric field exerts Lorentz body forces on its

self-induced charge distribution and drives electro-kinetic flow. We have investigated this electro-convective process for the general case of Debye thicknesses which are comparable with particle size. This case typically addresses the scenario of sub-micron particles in low-salt-concentration solutions. For particle size $a = 0.1$ μm, for example, the case $\lambda = 1$ corresponds to the salt concentration $n_\infty \approx 10$ μM, see (2.8).

The focus upon small particles allows an analytic weak-field investigation. It reveals a quadrupolar flow pattern, qualitatively similar to those found in thin-Debye-layer analyses. The global strength of this flow is quantified by the total 'inward flux' of liquid. This flux is the product of an $O(1)$ dimensionless constant F and $\epsilon a^3 E_\infty^2/\mu$.

It this paper we have employed the prototypical element of induced-charge electro-kinetics: a perfectly conducting spherical particle. Our work can be generalized to analyse dielectric particles as well. The driving mechanism for electro-convection – ionic impermeability of the particle and particle polarization – is the same in both cases. In the dielectric-particle case, however, the electric field must be solved inside the particle and then matched to that in the liquid through Gauss law. This procedure introduces a new parameter into the analysis, namely the fluid–particle ratio of dielectric constants. Since a dielectric particle possesses a finite polarizability, it is expected that the flow about it would be of smaller magnitude than that about a conducting particle, which is effectively infinitely polarizabile.

REFERENCES

Abramowitz, M. & Stegun, I. A. 1965 *Handbook of Mathematical Functions*, 3rd edn. Dover.

Ajdari, A. 2000 Pumping liquids using asymmetric electrode arrays. *Phys. Rev.* E **61** (1), R45–R48.

Bazant, M. Z. & Ben, Y. X. 2006 Theoretical prediction of fast 3D AC electro-osmotic pumps. *Lab on a Chip* **6** (11), 1455–1461.

Bazant, M. Z. & Squires, T. M. 2004 Induced-charge electrokinetic phenomena: Theory and microfluidic applications. *Phys. Rev. Lett.* **92** (6), 066101.

Ben, Y. X. & Chang, H. C. 2002 Nonlinear Smoluchowski slip velocity and micro-vortex generation. *J. Fluid Mech.* **461**, 229–238.

Brown, A. B. D., Smith, C. G. & Rennie, A. R. 2000 Pumping of water with ac electric fields applied to asymmetric pairs of microelectrodes. *Phys. Rev.* E **63** (1), 016305.

Happel, J. & Brenner, H. 1965 *Low Reynolds Number Hydrodynamics*. Prentice-Hall.

Levich, V. G. 1962 *Physicochemical Hydrodynamics*. Prentice-Hall.

Murtsovkin, V. A. 1996 Nonlinear flows near polarized disperse particles. *Colloid J.* **58** (3), 341–349.

Rubinstein, I. & Zaltzman, B. 2001 Electro-osmotic slip of the second kind and instability in concentration polarization at electrodialysis membranes. *Math. Mod. Meth. Appl. Sci.* **11** (2), 263–300.

Saintillan, D., Darve, E. & Shaqfeh, E. S. G. 2006 Hydrodynamic interactions in the induced-charge electrophoresis of colloidal rod dispersions. *J. Fluid Mech.* **563**, 223–259.

Saville, D. A. 1977 Electrokinetic effects with small particles. *Annu. Rev. Fluid Mech.* **9**, 321–337.

Shilov, V. N. & Simonova, T. S. 1981 Polarization of electric double-layer of disperse particles and dipolophoresis in a steady (DC) field. *Colloid J. USSR* **43** (1), 90–96.

Simonov, I. N. & Dukhin, S. S. 1973 Theory of electrophoresis of solid conducting particles in case of ideal polarization of a thin diffuse double-layer. *Kolloidnyi Z.* **35** (1), 191–193.

Simonova, T. S., Shilov, V. N. & Shramko, O. A. 2001 Low-frequency dielectrophoresis and the polarization interaction of uncharged spherical particles with an induced Debye atmosphere of arbitrary thickness. *Colloid J.* **63** (1), 108–115.

Squires, T. M. & Bazant, M. Z. 2004 Induced-charge electro-osmosis. *J. Fluid Mech.* **509**, 217–252.

Squires, T. M. & Bazant, M. Z. 2006 Breaking symmetries in induced-charge electro-osmosis and electrophoresis. *J. Fluid Mech.* **560**, 65–101.

Yariv, E. 2005 Induced-charge electrophoresis of nonspherical particles. *Phys. Fluids* **17** (5), 051702.